Romanian Reports in Physics, Vol. 66, No. 1, P. 200–211, 2014

ATTENUATION CORRECTION IN SPECT DURING IMAGE RECONSTRUCTION USING INVERSE MONTE CARLO METHOD A SIMULATION STUDY*

S. AHMADI[1], H. RAJABI[2], D. SARDARI[1], F. BABAPOUR[1], M. RAHMATPOUR[1]

[1] Faculty of Engineering, Science and Research Branch, Islamic Azad University, Tehran, Iran
E-mail: s_ahmadi597@yahoo.com; dsardari@hotmail.com; Farshid.mofrad@yahoo.com; msrn_62@yahoo.com
[2] Department of Medical Physics, Tarbiat Modares University, Tehran, Iran
E-mail: hrajabi@modarers.ac.ir

Received May 20, 2013

Abstract. The main goal of SPECT imaging is to determine the distribution of injected activity inside patient's body. However, due to photon attenuation, a quantitative study is encountered with remarkable error. Using Monte Carlo method, it is possible to find the most precise relationship between activity distribution and its projections. Therefore, it is impossible to create mathematical projections that include the effects of attenuation. This helps to have a more realistic comparison between mathematical and real projections, which is a necessary step for image reconstruction using MLEM.

Key words: Attenuation correction, Monte Carlo, MLEM.

1. INTRODUCTION

Radiography based on radio nuclides is one of the important applications of radioactive materials in nuclear medicine. The goal of radiography with SPECT is to obtain an accurate picture of the distribution pattern of labeled material in body [1]. For this purpose, the investigation of emitted radiations from Radionuclides is considered as an important issue.

During the detection process, various physical factors such as attenuation, scattering, and detector response influence on amount of emitted photons. Consequently this issue will effect on quality and accuracy of SPECT images.

If image reconstruction problem to be considered as a vector equation: $g = A f$; where g is vector of projection data, f is vector of activity distribution in body or unknown vector that must be reconstructed and A is transfer matrix (matrix of registration coefficients) [2]. Then the methods for solving this equation are divided into two types, analytic and iterative.

* Paper presented at the 1st Annual Conference of the Romanian Society of Hadrontherapy (ICRSH 2013), February 21–24, 2013, Predeal, Romania.

In analytical technique, the equation ($f = A–1g$) which is based on direct solution is used for finding the amount of vector f. This method has several major flaws: (a) $A–1$ doesn't exist; (b) if inverse matrix is available, needed computational operation is high. Therefore, in analytical methods the reconstruction of images is done by simplifying the matrix A, regardless of attenuation effect [3, 4].

In this method, it is assumed that pixel values in each projection are equal to the sum of activities that are located in front of pixel. So the inverse of radon transform is used for reconstructing the images. In terms of image processing, it is called filter back projection (FBP).

The images that are reconstructed based on FBP method have many disadvantages in quality and quantity aspects. The main reason of this problem is the effects of attenuation. Therefore, FBP is not an accurate method for quantification [5].

Another method for image reconstruction is iterative reconstruction. The major advantage of this method is that there is no need to calculate the inverse matrix. In this method unknown value f can be determined simply by inserting matrix A into algorithm's equations.

Iterative reconstruction methods are divided into two groups: The first group includes algebraic methods such as ART (Algebraic Reconstruction Technique), which images are reconstructed by solving the linear equations.

The second group is related to statistical reconstruction methods such as OSEM and MLEM. In these methods the operation of reconstruction of images is done *via* maximum likelihood algorithm. The most popular and widely studied of these iterative algorithms is the maximum likelihood expectation maximization (MLEM) algorithm, which models the Poisson noise inherent in single – photon data.

The algorithm that proposed by Lange and Carson is expressed by equation (1):

$$f_j^{k+1} = f_j^k \frac{1}{\sum_{i=1} a_{ij}} \sum_{i=1} a_{ij} \frac{g_i}{\sum_{j=1}^{m} a_{ij} f_j^k}. \tag{1}$$

In this equation: f_j^k, f_j^{k+1} are the initial estimates and later estimates respectively; n – number of pixels; g_i – measured projection; a_{ij} – matrix elements.

The most important factor in decreasing the quality of SPECT images is related to photons attenuation [7]. There are three methods for attenuation correction from the perspective of image reconstruction [8]. In the first method, images are reconstructed regardless of photons attenuation amount. This approximation is used in qualitative studies and isn't applicable in quantitative studies [9].

The second method for image reconstruction is done through attenuation simplification. In this method, attenuator material supposed to be uniform. But this isn't an accurate method because most part of body has unequal attenuation coefficient. Chang method is one of these methods that assumed a uniform attenuation

coefficient for tissues. For each pixel, correction factor can be calculated by averaging all projections toward that point. Subsequently final reconstructed image can be obtained by applying this factor in the initial image [10].

Another method for determining the attenuation map is using CT scan and entering the effects of attenuation coefficient in reconstruction equations. Generally in this case, the iterative algorithms are used for Image reconstruction [11–16].

The key element in MLEM algorithm is the system's probability matrix: a matrix that provides probabilities with witch each photon emitted from a pixel of the unknown image is detected. In probability matrix, the geometrical setup of system is taken into account. In addition, other physical parameters such as collimator response (in the case of SPECT), attenuation, scattering, etc. can be included [16, 17].

Since the main objective of this study is attenuation correction; then most important step in investigation of proposed method is applying attenuation effect on probability coefficients of the transform matrix. In other words, in this method the attenuation is effective in the production of transform matrix's elements. Dimensions of transform matrix depends on several factors, such as type of imaging (two or three dimensional), number of projection's angles and dimensions of the reconstructed image [18].

In nuclear medicine, instead of research on the images that obtained from patient's scan, simulated images could be studied. Regarding to statistical nature of factors that are effective in the process of nuclear imaging, the Monte Carlo code is used for simulation of these factors. By using this code, photon, related energy and other hardware factors which are effective in the process of SPECT imaging could be simulated. Generally, Monte Carlo' simulation codes are divided into two groups: general codes such as GEANT4, MCNP and EGS4 and specific codes for nuclear medicine such as SIMIND and SIMSET. In this study, SIMIND code is used for simulation of factors.

2. MATERIALS AND METHODS

The proposed method includes four steps: (a) simulation of imaging system, (b) obtaining the transform matrix, (c) production of simulated projections and (d) image reconstruction. In the following, each step will be described in detail.

2.1. SIMULATION OF SYSTEM AND PHANTOMS

In this study, SIMIND code (version 4.8) was used [19]. The parameters of this simulator involves the use of low energy and general purpose collimator, NaI crystal with thickness of 0.95 cm, low energy window of 126 to 154 Kev. Also camera's turning range was assumed to be 30 cm. Imaging was carried out using

64 angles and images were stored in 64×64 matrices. Another point is that, these results can be generalized to other drugs, and only the attenuation map of other energies must be used in the algorithm.

2.2. OBTAINING OF THE TRANSFORM MATRIX PROBABILITY MATRIX

In order to obtain transform matrix, uniform activity phantom (as unit input) with attenuated phantom (which the attenuation correction operation will be carried out for this specific phantom) are given to the Monte Carlo simulation code (SIMIND). In the final step of simulation, LMF file as one of the output files will be produced. This file includes information about the history of each photon (the exact location of emission, related energy, last location of scattering, the location of registering). Using this file and MATLAB simulator the transform matrix could be determined.

It is clear that, when the number of samples is high enough, then the relative frequency indicates the probability coefficient. So, by inserting the uniform activity phantom which includes high activity level, then matrix A could be determined with more accuracy. Let' s suppose i indicates the photon radiation voxel position and j represents the pixel location, in that case elements of matrix A, a_{ij}, determines the relationship between j^{th} pixel in the image with ith voxel in the activity distribution. In other words, element, a_{ij} indicates the probability of registration of emitted photon from ith voxel into jth pixel.

In the next step, regardless of attenuation, by inserting zero in the elements of attenuation phantom and use of uniform activity phantom and LMF data, which was created as previous steps, matrix A was produced. This transform matrix will be used to reconstruct the reference image and image reconstruction with MLEM method without attenuation correction. Using simulations, this study was carried out in two parts: simple geometric phantom and four-dimensional human body phantom (NCAT) [20].

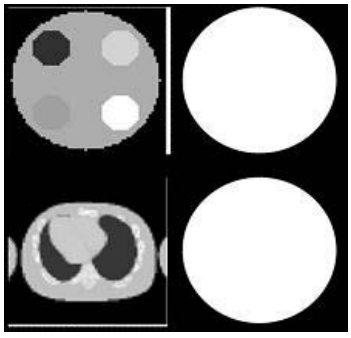

Fig. 1 – Cross section images of the phantom used to generate the transform matrix: top – phantom geometry, low: slice of the NCAT phantom; right – unit activity phantom, Left: the actual attenuation map.

2.3. CREATION OF SIMULATED PROJECTIONS

At this stage, activity and attenuation phantoms are given to the SIMIND code as input. And simulated projections are produced. Also, in this study, simple activity phantom was used in both uniform and non-uniform activity (Fig. 2).

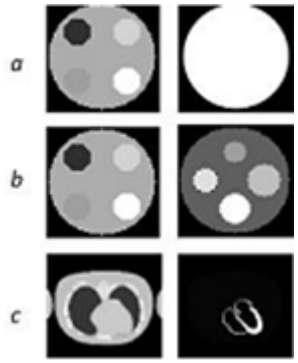

Fig. 2 – Cross section images of the phantom that are used for production of simulated projections: a) simple phantom with uniform activity; b) simple phantom with non-uniform activity; c) slice of the NCAT phantom, Right: distribution of activity, Left: the attenuation map.

2.4. RECONSTRUCTION OF TEST PHANTOM IMAGES BY MLEM RECONSTRUCTION ALGORITHM

After producing the transform matrix and simulated projections in the first and second stages, in the third step, image reconstruction is carried out by MLEM algorithm.

According to the MLEM algorithm the corrective value is produced through dividing the measured projection by mathematical projection (mathematical projection was produced through multiplying the initial estimate by the transform matrix).

This corrective value is used for updating the initial estimation. Because in the proposed method, for producing of the transform matrix (A), attenuation coefficients have been effective, so it is predictable that more accurate comparison will be happened between measured and mathematical projections. Subsequently, more accurate correction factor is available for updating the initial estimation. Thus attenuation correction will be applicable in the process of image reconstruction.

For quantitative investigation of the proposed method and to compare it with conventional reconstruction methods, we need a reference image that there are not attenuation effects on it.

To create a reference image, the attenuation phantom was considered zero. Using transform matrix without attenuation effects and simulated projections with

zero attenuation phantom, the reference image was reconstructed. For evaluation of different regions of the image, by drawing the same ROI in different regions of the reconstructed images, the mean pixel values were determined (Fig. 3).

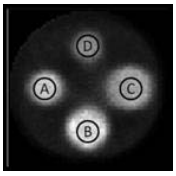

Fig. 3 – Drawing a ROI in different regions of the image to calculate the average pixel values.

3. RESULTS

3.1. THE RESULTS OF THE RECONSTRUCTION OF THE PHANTOM WITH UNIFORM ACTIVITY DISTRIBUTION

Visual and qualitative assessment is one of simplest and primitive comparison methods for quality evaluation of images. But only when the difference between images is obvious, this method is applicable. The reconstructed images produced by proposed method, MLEM without attenuation correction, and FBP method are compared qualitatively in Fig. 4.

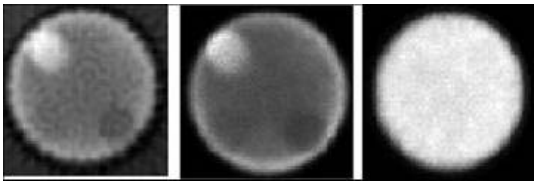

Fig. 4 – The reconstructed images for uniform activity phantom with non-uniform attenuation from left to right: by proposed method, MLEM without attenuation correction method, FBP without attenuation correction method.

Attenuation effects are completely obvious in the images that were reconstructed with MLEM method without attenuation correction and FBP method. So where the amount of attenuation in the attenuation phantom is low and high, these effects in the reconstructed image appear as bright and dark spots respectively. On the other hand, attenuation effects were corrected completely in the images reconstructed by proposed method and background has a uniform activity. In Fig. 5, the diagram of pixel values in terms of pixel number for images reconstructed from simple geometrical phantom in three modes (reference, proposed method and MLEM method without attenuation correction reconstruction) has been shown.

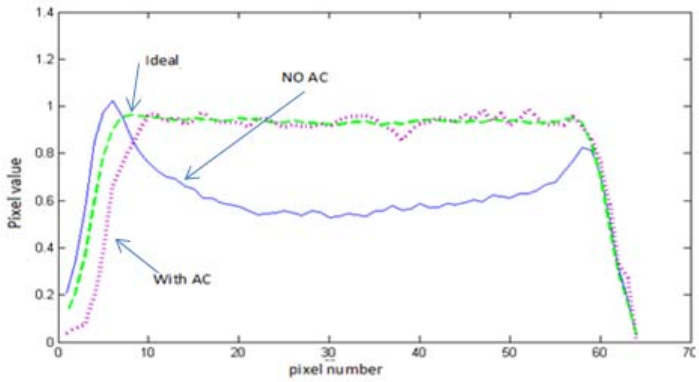

Fig. 5 –The diagram of Pixel values in term of pixel number for images reconstructed from simple geometrical phantom in three cases (reference, proposed method, and MLEM without attenuation correction reconstruction).

The results that obtained from quantitative evaluation of Fig. 5 could be expressed as follows:

As expected the reconstruction image by proposed method has a uniform distribution of pixel values, and the numerical value of pixels for reconstructed image by proposed method is equal to pixels numeric value in the reconstructed reference image. And equality of these amounts indicates that attenuation has been corrected completely, while in MLEM method without attenuation correction the amount of the fixed distribution has been declined significantly in central parts because of attenuation.

3.2. THE RESULTS FROM RECONSTRUCTION OF THE PHANTOM WITH NON-UNIFORM ACTIVITY DISTRIBUTION

The images of simulated phantom scan with non-uniform activity distribution, which were reconstructed by MLEM with attenuation correction, MLEM without attenuation correction and FBP methods are shown in Fig. 6. This illustrates that attenuation effects are completely evident in the reconstructed images by previous method, while in the proposed method, there is no sign of attenuation in the reconstructed images.

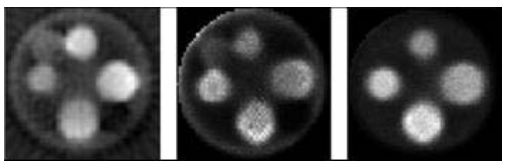

Fig. 6 – The reconstructed images from the non-uniform activity phantom and non-uniform attenuation. From right to left: proposed method, MLEM without attenuation correction, and FBP without attenuation correction method.

From Fig. 7, it is completely clear that on the pixel numerical values diagram, in the proposed method, the numerical values related to reconstructed image are perfectly corresponded to the reference image and the negligible difference is only related to noise that in the process of image reconstruction is unavoidable. Also this diagram explains that in attenuation correction method during the image reconstruction contrast value has not changed in comparison with the reference diagram.

On the other hand, the images obtained from the reconstruction without attenuation correction has less contrast in comparison with the reference diagram. This means that the numerical value between background and circles do not have much difference, and this lack of difference is related to the attenuation effect. Table 1 shows the results of three states: reference image, the reconstructed images with and without attenuation correction.

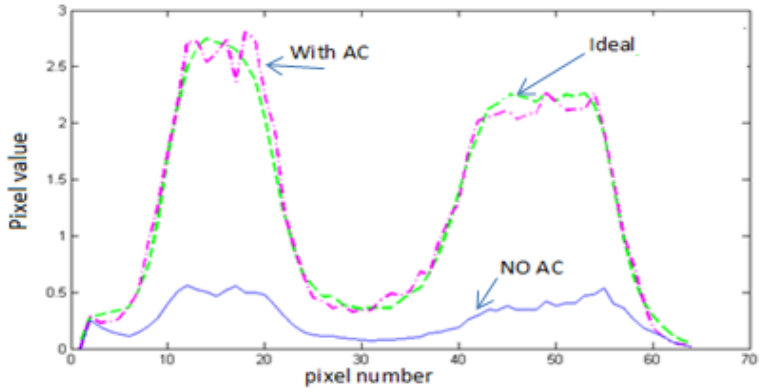

Fig. 7 – Pixel values profile of simple geometric phantom for images that reconstructed for non-uniform distribution of activity and attenuation in three states: MLEM with and without attenuation correction and reference image.

In Fig. 7 letters A to D Show ROI areas in this study Comparison of the obtained results in three cases indicates that numerical values of circles in the proposed method are very close to the reference case. On the other hand, there is a noticeable difference between the values of reconstruction without attenuation correction and the reference case.

Table 1

The average value of pixels in four different parts of geometric non-uniform activity phantom image for reference, corrected and uncorrected attenuation effect

Case Study	A	B	C	D	BG
Reference image reconstructed by MLEM	1.99	2.40	2	1.30	0.39
Reconstructed images without attenuation correction	0.36	0.47	0.43	0.30	0.08
Image reconstruction by proposed method	1.97	2.34	1.67	1.10	0.38

3.3. THE RESULTS OF NCAT PHANTOM IMAGES RECONSTRUCTION

In Fig. 8, the results of reconstruction of images for NCAT phantom using proposed method, reconstruction without attenuation correction, and FBP have been shown, but before correction there are two issues for the NCAT phantom images:

1. Although activity levels in the lung and its field are the same, lungs are slightly brighter than the background mistakenly.

2. Due to less activity attenuation that has occurred in surface than the depth of body, skin's activity has more level.

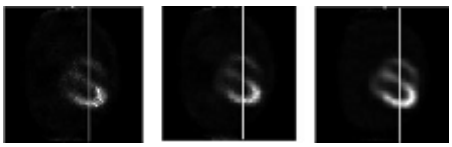

Fig. 8 – From left to right: reference image reconstructed using the proposed method, the reconstructed image using the proposed method, the reconstructed images without attenuation correction.

Figure 9 shows the profile of pixel values related to a row of reconstructed images in the reference case, with and without attenuation correction. In quantitative analysis of Fig. 9 and comparison of these three profiles, following results obtained:

First, the profile of reference image and the one belongs to the image reconstructed by proposed method have similar numerical values and contrasts.

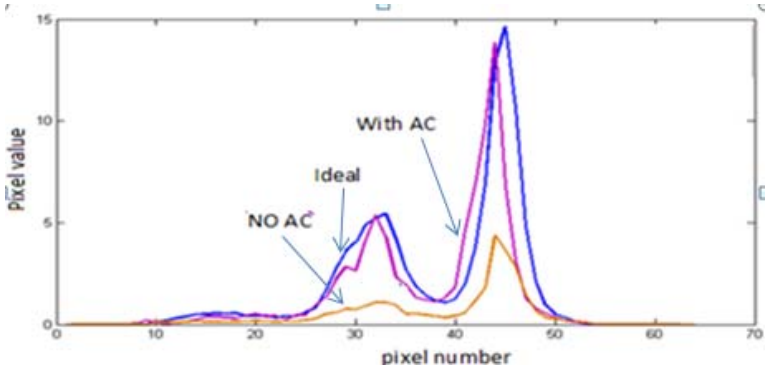

Fig. 9 – The reconstructed image without attenuation correction has less numerical values and contrast than the reference case and the images with attenuation correction during reconstruction.

Accuracy of matrix A depends on input unit activity levels. So, if activity level be in high level, then matrix A would be more accurate. On the other hand, by increasing the level of input unit activity, the time needed for calculation of matrix A would increase. Consequently, to produce the matrix A in less time and in

acceptable accuracy for input unit with activity of 50, 100, 200, 300 million Becquerel the reconstructed images are shown in Fig. 10.

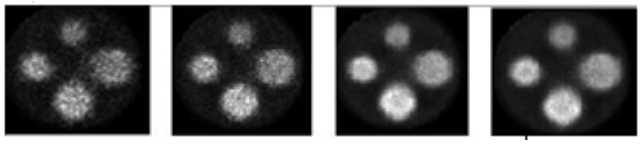

Fig. 10 – The reconstructed images using matrix *A* with different activities as input unit: from right to left: activity 300, activity 200, activity 100, and activity 50 million Becquerel.

4. DISCUSSION AND CONCLUSION

The current study aimed to propose a new method to correct attenuation. Now, there are many ways to correct attenuation. Diagnosis use of most of the methods is ambiguous and researchers attempt to find a comprehensive method for complete and precise correlation of attenuation. In the previous methods as Chang (10), the primary reconstruction of the image is done. Then by space attenuation coefficient, assuming the uniformity of attenuating space, attenuation correction factor is obtained and by applying this factor on the reconstructed primary image, attenuation correction is done. In the current study, there is no need for uniformity of attenuating space. The number of voxels and pixels are 64×64. For each voxel, photon is radiated of it, there is 64×64 record location in pixel possibly and as the number of voxels is 64×64, matrix A applied for activity distribution phantoms and attenuation has 4 096×4 096 components. Based on the number of the elements of this matrix, matrix *A* production stages has high computing value and it is time-consuming. Thus, 2-D activity phantom is considered in this study to reduce calculations volume and time. Thus, the investigation of the proposed method on 2-D phantoms with bigger size (more pixel and voxels) and 3-D phantoms required high speed and high memory computers.

In all the cases, in producing matrix A, activity phantom is applied uniformly as in the identification of each system and its performance, a unique input is considered for it. The important point is determining the unit input value. Because if it is not big enough, the probability matrix will not have the adequate accuracy and the image is including high noise.

As it is shown in charts 11, by the increase of input activity in obtaining matrix A, the probability coefficients are more accurate and the noise is reduced. In other words, as it was said before, the calculation and production due to its high volume is time-consuming where matrix *A* is increased with the increase of unit input. The required time for calculation of *A* based on activity value is shown in Table 2.

Table 2

Calculation tine of matrix A base on activity of activity phantom in Mega Becquerel in matrix *A* production

The amount of input activity	Time [min]
50	90
100	190
200	340
250	550

By considering time table of matrix *A* production and comparing the charts 10, 11, it is observed that there is no significant difference between the images of activity 200, 250 Megabecquerel, but there is a significant difference between calculation time of the matrix at activity mode 200, 250 (more than 3 hours). It seems that the appropriate activity for input phantom is 200.

The matrix of probability coefficients obtained by this method needs more volume for storing. This matrix in 2-D state has 4 096×4 096 elements and if for storing each element, 2 bits are required, the total required volume is about 33 megabite. Thus, the required volume for storing and calculation time of this method for the case in which phantom size is more than 64×64, it is increased considerably. This method for 3-D and even 2-D with phantom size more than 64×64 is impossible.

It is possible to make optimized changes with more research about storing and calculation time of this matrix, it can be expected that by removing these limitations, we achieve the best results in application of the method.

***Acknowledgements*.** The applied simulator code in this study was written by Professor Michele Liongberg from Lond University of Sweden. My gratitude goes to him to add the data presentation on as list mode that was done in accordance with the request of the authors.

REFERENCE

1. Beriner D.R., *Nuclear Medicine; Technology and Techniques*, 3rd Edition, 1994.
2. Anger H., *Scintillation camera*, Rev. Sci. Instruction, 195829, 27–33, Jerrold T. Bushberg, *The Essential physics of medical imaging*, 1994, 527–580.
3. Freeman L., *Clinical radionuclide imaging*, 3rd edition, United states of America, 1984, 13, 254.
4. Jerrold T. Bushberg, *The essential physics of medical imaging*, 527–580, 1994.
5. Philippe P. Bruyant, *Analytic and Iterative Reconstruction Algorithms in SPECT*, J. Nucl. Med., **43**, 1343–1358 (2002).
6. Shepp LA, Vardi Y., *Maximum likelihood reconstruction for emission tomography*, IEEE Trans. Med. Imaging, **MI-1**, 113–122 (1982).
7. Keramer E. L., Sanger J.J., *Clinical SPECT Imaging*, Raven Press, Ltd, New York, 1995.
8. Cherry S., Sorenson J., Phelps. M., *Physics in Nuclear Medicine*, 3th edition, Philadelphia, Pennsylvania, 2003.

9. Zeng G.L., *Image reconstruction – A tutorial*, Comput. Med. Imaging Graph., **25**, 97–103 (2001).
10. Lange K., Bahn M., Little R., *A theoretical study of some maximum likelihood algorithms for emission and transmission tomography*, IEEE Trans. Med. Imaging., **62**, 106–14 (1987).
11. Tsui B.M.W., Hu H.-B., Gilland D.R., Gullberg G.T., *Implementation of simultaneous attenuation and detector response correction in SPECT*, IEEE Trans Nucl Sci., **NS-35**, 778–83, (1988).
12. Gullberg G.T., Huesman R.H., Malko J.A., Pelc N.J., Budinger T.F., *An attenuated projector-backprojector for iterative SPECT reconstruction*, Phys. Med. Biol., **30**, 799–815 (1985).
13. Floyd Jr C.E., Jaszczak R.J., Greer K.L., Coleman RE., *Inverse Monte Carlo as a unified reconstruction algorithm for ECT*, J. Nucl. Med., **27**, *10*, 1577–85 (1986).
14. Ortuno J.E., Kontaxakis G., Guerra P., Santos A., *3D-OSEM transition matrix for high resolution PET Imaging with modeling of the gamma-event detection*, 2005 IEEE NSS-MIC Conference, Puerto Rico, Conference Record, October 2005.
15. Motta A., Damiani C., Del Guerra A., Di Domenico G., Zavattini G., *Use of a fast EM algorithm for 3D image reconstruction with the YAP-PET tomography*, Computerized Medical Imaging and Graphics, **26**, *10*, 293–302 (2002).
16. George K. Loudos, *An efficient analytical calculation of probability matrix in 2D SPECT*, Computerized Medical Imaging and Graphics, **32**, 83–94 (2008).
17. Chang.L., *Attenuation correction and in complete projection in SPECT*, IEEE, **26**, 2780 (1979).
18. James A. Patton and Timothy G. Turkington, *SPECT/CT Physical Principles and Attenuation Correction*, Journal of Nuclear Medicine Technology, 2008, pp. 1–10.
19. www 2.msf.lu.se/simind/simind.pdf
20. Segars Wp., Development of a new dynamic NURBS – based cardiac torso (NCAT) Phantom, 2001.